J Solid State Electrochem (2012) 16:2691–2698
DOI 10.1007/s10008-012-1672-0

ORIGINAL PAPER

The synthesis of nitrogen-doped carbon nanotubes/gold composites and their application to the detection of thioridazine

Xiaomiao Feng · Chen Wang · Rongjing Cui · Xiaoyan Yang · Wenhua Hou

Received: 15 September 2011 / Revised: 7 January 2012 / Accepted: 30 January 2012 / Published online: 1 March 2012

Abstract Nitrogen-doped carbon nanotubes (N-CNTs)/gold composites were synthesized through a simple self-assembly method. The morphology, composition, and optical properties of the resulted composites were investigated by transmission electron microscopy, scanning electron microscopy, X-ray diffraction, Raman spectra, ultraviolet–visible absorption spectrum, and X-ray photoelectron spectroscopic. This nanocomposite combines the advantages of N-CNTs and gold nanoparticales showing many excellent properties such as good dispersibility in water and satisfactory biocompatibility. Cyclic voltammogram experiment shows that N-CNTs/gold composite has high conductivity. Based on these aspects, N-CNTs/gold-modified electrode was applied to the voltammetric determination of thioridazine hydrochloride (TH) successfully. The linear calibration range for the TH sensor was 12~850 μM with a detection limit of 1.3 μM at a signal-to-noise ratio of 3, long-term stability, and good reproducibility.

Keywords Nitrogen-doped carbon nanotubes · Gold · Thioridazine · Electrochemical sensor

X. Feng (✉)
Key Laboratory for Organic Electronics and Information Displays, Institute of Advanced Materials, School of Materials Science and Engineering, Nanjing University of Posts and Telecommunications,
Nanjing 210046, China
e-mail: iamxmfeng@njupt.edu.cn

C. Wang · R. Cui (✉)
Jiangsu Laboratory of Advanced Functional Materials, Department of Chemistry and Materials Engineering, Changshu Institute of Technology,
Changshu 215500, China
e-mail: rongjingcui@gmail.com

X. Yang · W. Hou
Key Laboratory of Mesoscopic Chemistry and Key Laboratory of Analytical Chemistry for Life Science, School of Chemistry and Chemical Engineering, Nanjing University,
Nanjing 210093, China

Introduction

Since the discovery of carbon nanotubes (CNTs) [1], they have received great interest because of their unique structural, electrical, and mechanical properties. To date, CNTs have shown promising application prospect in many fields, such as field emission displays and radiation source, conductive and high-strength composites, nanoscale semiconductor devices, sensors, energy storage devices, and hydrogen storage media [2–8]. To optimize the use of CNTs in many of these applications, especially in sensors, it is necessary to functionalize CNTs with polymers, guest molecules, or side wall substituents for improving the biocompatibility because of the hydrophobicity CNTs surface [9]. However, the complete graphene structure and relatively less defect sites on the CNTs limited the introduction of the side wall substituents. Recently, it has been reported that CNTs doped with heteroatom, such as boron and nitrogen can overcome these shortcomings [10]. The doping of heteroatom to some extent undermines the ordered structure of CNTs and creates many defect sites on the wall. The curvature changes the chemically inert graphite surface and makes it easier to incorporate atoms on the tube surface. Especially, nitrogen-doped carbon nanotubes (N-CNTs) has higher conductivity and better biocompatibility than the pure CNTs, which are extremely attractive as important nanomaterials in sensors [11–13].

Electrochemical sensors have been widely applied to detect various substances because of their high sensitivity and desirable selectivity. Generally, the detection of substances based on electrochemical sensors realized by surface modification of electrodes, which can optimize the surface state of the electrodes, reduces the overpotential and increases the rate of electron transfer process. This detection method is very simple and nontoxic. Electrochemical sensors based on CNTs provide an interesting alternative for quantification of many analytes due to their unique one-dimensional hollow nanostructure, high-aspect ratios of the tubes, and unusual properties. CNTs application in electrochemical sensors is expected to be enhanced by CNTs/metal nanoparticles (NPs). The dispersion of metal NPs on the CNTs wall potentially provides a new way to develop catalytic and optoelectronic materials. Particularly, gold NPs have received a great deal of attention because of their unique electrical and optical properties as well as extensive applications [14]. The synthesis and application in electrochemistry of gold NPs functionalized CNTs have been intensively studied [8, 15, 16]. However, the application of N-CNTs/gold composite in electrochemical sensors has been rarely reported.

Thioridazine hydrochloride (TH), the hydrochloride of 10-[2-(lmethyl- 2-piper-idyl)ethyl]-2-methylthiophenothiazine, is a phenothiazine neuroleptic drug used for the treatment of schizophrenia, other psychiatric disorders, and the short-term treatment of adults with major depression who have varying degrees of associated anxiety. The serious side effect of TH is the potentially fatal narcoleptics malignant syndrome. Therefore, it is significant to establish a simple and sensitive method for its determination due to the clinical importance of TH. To date, some analytical methods have been reported for determination of TH, such as high-performance liquid chromatography, capillary electrophoresis, chemiluminescence, and flow-injection on-line oxidizing fluorimetry [17–20].

In the present work, N-CNTs/gold NPs composites were synthesized through a simple self-assembly method. The morphology, composition, and optical properties of the resulted composites were investigated by transmission electron microscopy (TEM), scanning electron microscopy (SEM), Raman, ultraviolet–visible (UV–Vis) absorption spectrum, and X-ray photoelectron spectroscopic (XPS). This nanocomposite combines the advantages of N-CNTs and Au NPs showing many excellent properties such as good solubility, dispersibility in water, and satisfactory biocompatibility. Based on these aspects, it was a modified electrode and applied to the voltammetric determination of TH successfully. This detective system is very simple, effective, and fast, which has great potential application in a clinic.

Experimental

Reagents

Trisodium citrate, KBH_4, NaCl, and $HAuC1_4$ were purchased from the Shanghai Chemical Reagent Company. TH and poly (diallyldimethylammonium chloride) (PDDA, 20%, *w*/*w* in water, MW=200,000–350,000) was from Sigma-Aldrich Chemical Co. All other reagents were of analytical grade and used without further purification.

Synthesis of N-CNTs/gold NPs composite

The gold colloid was prepared by reducing $HAuC1_4$ aqueous solution with trisodium citrate and KBH_4 [21]. The average diameter of the prepared gold NPs is about 5 nm. N-CNTs was synthesized by chemical vapor deposition at 650 °C and pyridine was employed as a precursor and then purified as described in a previous report [22]. The purified N-CNTs were treated by refluxing in concentrated nitric acid solution at 110 °C for 6 h. The suspension was centrifuged and washed with double-distilled water till the pH value of the filtrate reached 7.0. The obtained solid was redispersed in water with a concentration of 2.5 mg mL^{-1}. The N-CNTs suspension was then mixed with a cationic polyelectrolyte, PDDA, and NaCl aqueous solution under stirring for 30 min. PDDA was adsorbed to the surface of N-CNTs due to the electrostatic interaction between the carboxyl groups and the polyelectrolyte. After filtration and thorough washing with deionized water, the PDDA-modified N-CNTs were mixed with gold colloid for 30 min. The negatively charged gold NPs were anchored to the surface of PDDA-modified N-CNTs through the electrostatic interaction between the polyelectrolyte and gold NPs. The final product was centrifuged and washed with distilled water and ethanol and then dried in a vacuum overnight at 60 °C.

Preparation of N-CNTs/gold NPs-modified glassy carbon electrode

The glassy carbon electrodes (GCE, 3 mm in diameter) were polished with 1.0, 0.3, and 0.05-μm alumina slurry followed by a rinse with double-distilled water, and then allowed to dry at room temperature.

The N-CNTs/gold was dispersed in distilled water to form a 2.0-mg mL^{-1} solution under ultrasonication. The resultant colloidal solution (5 μL) was then dropped onto the pretreated GCE surface and allowed to dry under ambient conditions.

Characterization

The morphologies were investigated by TEM (JEOLJEM-200CX) and SEM (LEO1530VP). X-ray diffraction (XRD) patterns were obtained on a Philip-X'Pert X-ray diffractometer. Resonance Raman spectra were recorded on a Renishaw-inVia Raman microscope (Renishaw, UK). UV–Vis absorption spectrum was recorded on a UV-2401PC spectrometer. XPS analysis was performed on an ESCALAB MK II X-ray photoelectron spectrometer. Electrochemical experiments were conducted with a CHI660C workstation (Shanghai Chenhua, Shanghai). All experiments were carried out using a conventional three-electrode system in 0.1-M phosphate buffer solution (PBS), where nanocomposite-modified GCE was used as the working electrode, a platinum wire as the auxiliary electrode, and a saturated calomel electrode as the reference electrode.

Results and discussion

N-CNTs/gold composites have been successfully synthesized by a self-assembly method in the presence of PDDA. Figure 1a, c shows the TEM and SEM images of N-CNTs, respectively. They display a well-defined one-dimensional structure with smooth surface, and the outer diameter range from 20 to 40 nm. The surface of the nanotubes becomes rough after the modification of gold NPs, as shown in Fig. 1b, d. The outside particles in Fig. 1d and the corresponding dark spots in Fig. 1b are gold NPs. Most of the N-CNTs are adsorbed by gold NPs with an average diameter of 5 nm, indicating that gold NPs are successfully modified onto the N-CNTs surface.

Figure 2 displays the XRD pattern of N-CNTs/gold composites. From the figure, we can see the peak at 25.86° arised from the (002) plane of graphite in the N-CNTs. In the figure, besides the N-CNTs peak, four additional peaks at 38.23°, 44.26°, 64.70°, and 77.49° representing Bragg reflections from (111), (200), (220), to (311) planes of gold are observed, showing the existence of gold NPs in the N-CNTs/gold composite. Crystallite sizes are calculated from the Au(111) diffraction line using Scherrer's equation, $L = k\lambda/\beta \cos\theta$, where L is the mean dimension of the crystallites, β is the full width at half maximum of the diffraction peak, θ is the diffraction angle, λ is the wavelength of the CuKα radiation (0.1540 nm), and k is equal to 0.89 [23]. The calculated average size of gold in the composite is about 5.5 nm, which is in agreement with the results of TEM and SEM (Fig. 1b, d).

The XPS confirms the doping of N species and the presence of gold NPs in the composites too. From the wide

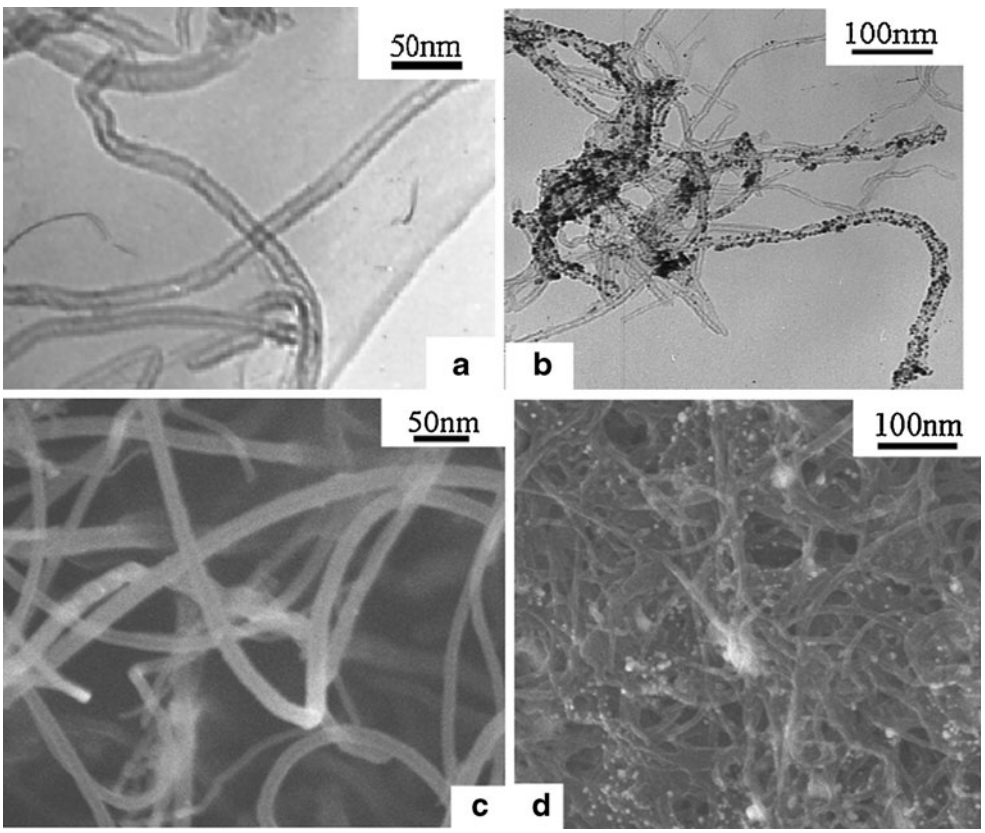

Fig. 1 TEM (**a**, **b**) and SEM (**c**, **d**) images of N-CNTs (**a**, **c**) and N-CNTs/Au (**b**, **d**)

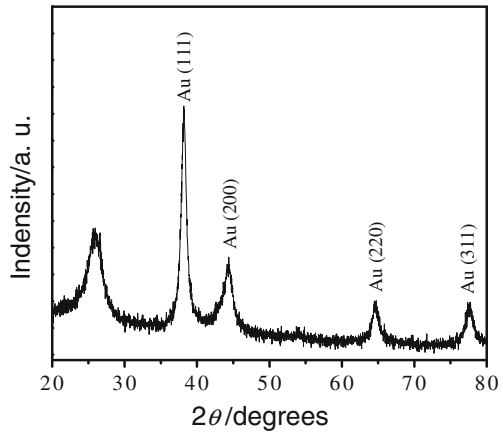

Fig. 2 XRD pattern of N-CNTs/Au

scan XPS spectrum of N-CNTs/gold shown in Fig. 3a, the peak at 84 eV corresponds to Au 4f indicating the presence of gold. The N1s XPS of N-CNTs/gold consisted of two peaks assigned to the pyridinic and graphitic nitrogen atoms at 399.5 and 402.4 eV, respectively (Fig. 3b). The N atom content of the N-CNTs is about of 5.0%.

Raman spectrum is a very useful non-destructive tool to characterize carbon-based materials, especially for distinguishing ordered and disordered carbon structures. In the Raman spectrum of N-CNTs (Fig. 4a), the peak centered at 1349 cm^{-1} is the Raman active D-band and the other centered at 1593 cm^{-1} is the Raman active G-band. The D-band can be explained as disorder-induced features due to the finite particle size effect or lattice distortion. The G-band originates from the Raman active E_{2g} mode due to in-plane atomic displacements [24]. In addition, the derived intensity ratio of the D-band to G-band (I_D/I_G) indicates the disorder or decrease in the average size of the sp^2 domains of N-CNTs. The intensity ratio I_D/I_G is 0.92, which is much higher than 0.24 for undoped CNTs [25], illustrating that the nitrogen doping is very effective in introducing defects into the structure of the CNTs. After the decoration of gold NPs, the D-band is shifted to 1,360 cm^{-1} because of the interaction of N-CNTs and gold. Whereas the intensity of G-band at 1,593 cm^{-1} increases dramatically due to the strong surface enhancement effects of gold NPs [26].

UV–Vis absorption spectra of gold, N-CNTs/gold, and N-CNTs are shown in Fig. 5. It can be seen that the acid-treated N-CNTs has a maximum peak at about 255 nm (Fig. 5c), which is a clear diagnostic of covalent side wall functionalization, i.e., disruption of the conjugated π system [27]. The characteristic peak of citrate-stabilized colloidal gold NPs appears at 518 nm (Fig. 5a), which is caused by the surface plasmon resonance. Figure 5b shows the UV–Vis spectrum of N-CNTs/gold nanocomposites. Both the characteristic peaks of N-CNTs and colloidal gold NPs can be seen in the figure. However, the absorption peak intensity

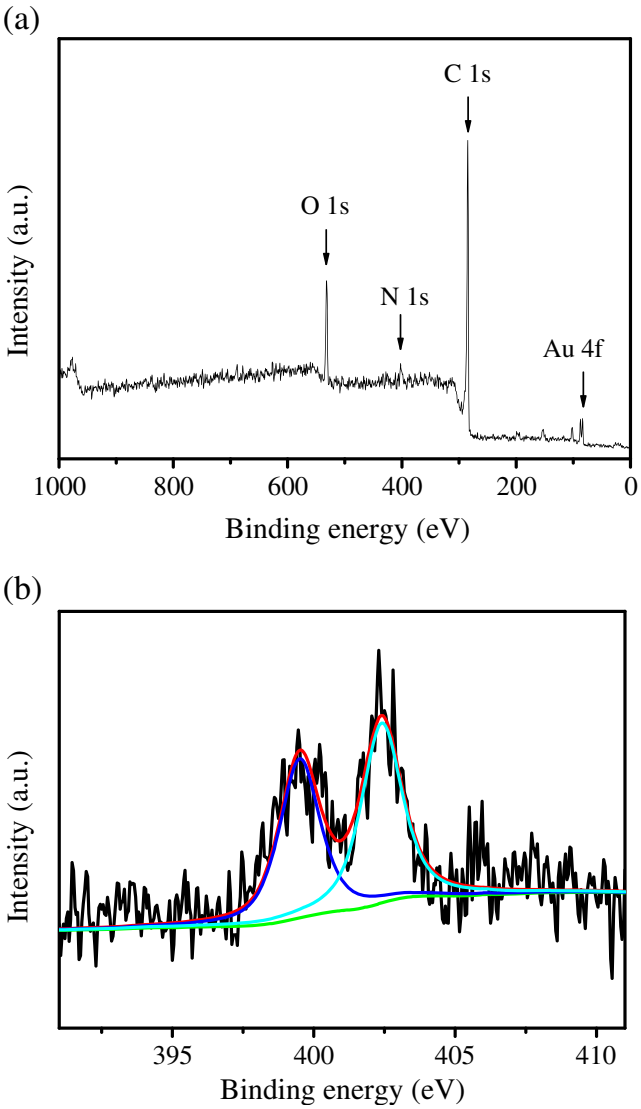

Fig. 3 Wide-range XPS of N-CNTs/Au (**a**) and high resolution N (*1 s*) spectra of N-CNTs/Au (**b**)

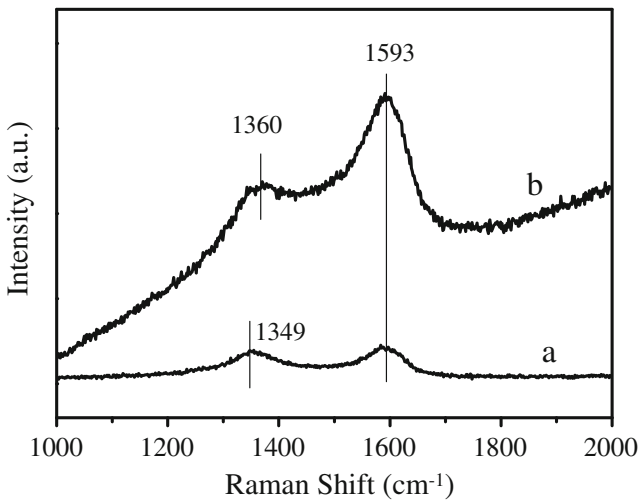

Fig. 4 Raman spectra of N-CNTs (**a**) and N-CNTs/Au (**b**)

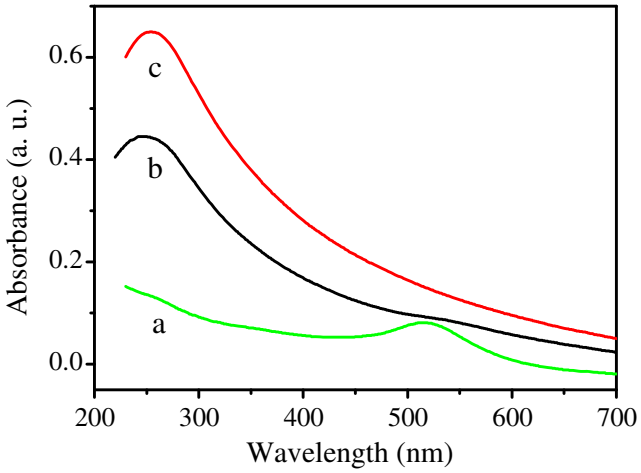

Fig. 5 UV spectra of Au (**a**), N-CNTs/Au (**b**), and N-CNTs (**c**)

of colloidal gold NPs is very weak. There are two possible reasons leading to this phenomenon. Firstly, it may be covered by the strong absorption peak of N-CNTs in the same region. Secondly, it is well known that the surface plasmon resonance bands of metal NPs are sensitive to their surrounding environment [28]. The different environment between N-CNTs/gold NPs and colloidal gold NPs may result in the diminishing of the gold NPs peak in the N-CNTs/gold composite.

Figure 6 shows the cyclic voltammograms (CVs) of bare GEC, pure CNTs-, N-CNTs-, and N-CNTs/gold-modified GCE in 0.1 M pH 6.0 PBS in the presence of 1.0×10^{-4} M TH, respectively. There is a very small oxidative peak for TH of the bare GCE. The oxidative peak is increased obviously after the electrodes are modified by pure CNTs and N-CNTs. Moreover, the increased degree of oxidative peak for

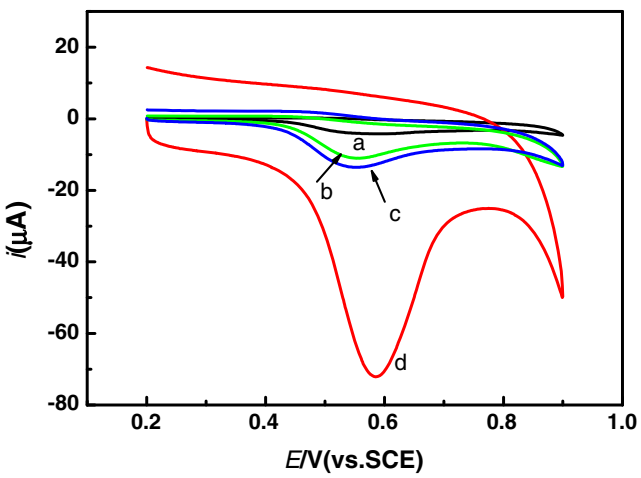

Fig. 6 CVs of **a** bare GEC, **b** pure CNTs-, **c** N-CNTs-, and **d** N-CNTs/gold-modified GCE in 0.1 M pH 6.0 PBS containing 1.0×10^{-4} M TH, respectively

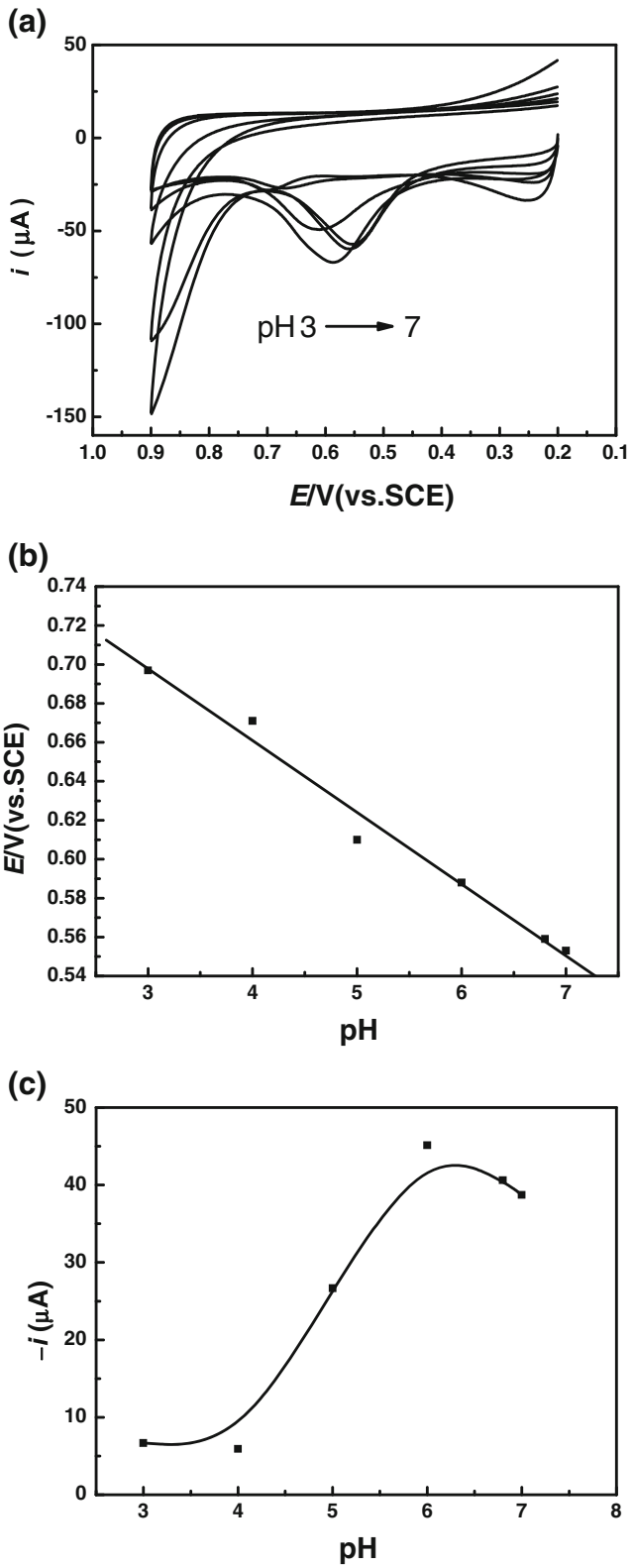

Fig.7 CVs of N-CNTs/gold-modified GCE in different pH PBS (3, 4, 5, 6, 6.8, and 7) containing 1.0×10^{-4} M TH (**a**); the relationship of the oxidation peak potential (**b**) and the oxidation peak current (**c**) with pH value

N-CNTs-modified GCE is higher than that of pure CNTs-modified GCE which may be caused by the excellent properties of N-CNTs. Especially, The peak current of TH for the N-CNTs/gold-modified GCE shows a remarkable value which is much larger than that of the above, indicating that gold can improve the catalytic activity for the oxidation of TH effectively.

The effect of pH on the oxidation peak potential and peak current of TH is studied using CVs, as shown in Fig. 7. With the increase of pH value in the range from 3.0 to 7.0, the oxidation peak potential of TH shifts towards a more negative value. The linear equation as follows:

$$E_{p,a}/V = 0.80839 - 0.03687\ pH\ (R = 0.99)$$

The corresponding slope is 0.03687 V/pH, suggesting one-proton process coupled with two electrons reaction of TH. The oxidation peak current first increases with the increasing of pH value. When the pH value is of 6.0, it reaches the maximal value. If the pH value continues to increase, the peak current will deduce. Therefore, pH 6.0 is the optimal one to the detection of RH.

Figure 8 shows the CVs of the N-CNTs/gold-modified GCE containing 1.0×10^{-4} M TH in pH 6.0 PBS at different scan rates from 100 to 450 mV/s. With the increase of scan rate, the peak potential shifts in positive direction. No cathodic peak is observed on the reverse scan at all the potential, indicating irreversible

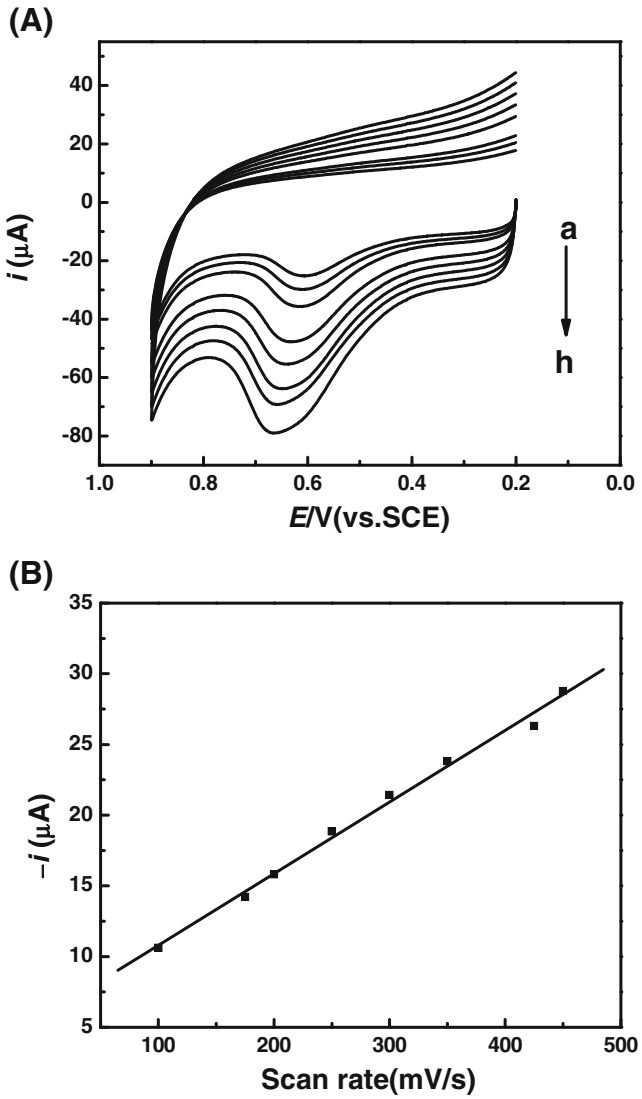

Fig. 8 Effect of scan rate on the CVs of N-CNTs/gold-modified GCE in pH 6.0 PBS at 100, 175, 200, 250, 300, 350, 425, and 450 mV/s containing 1.0×10^{-4} M TH (*from inner to outer*) (**a**). Plots of anodic peak current vs. scan rates (**b**)

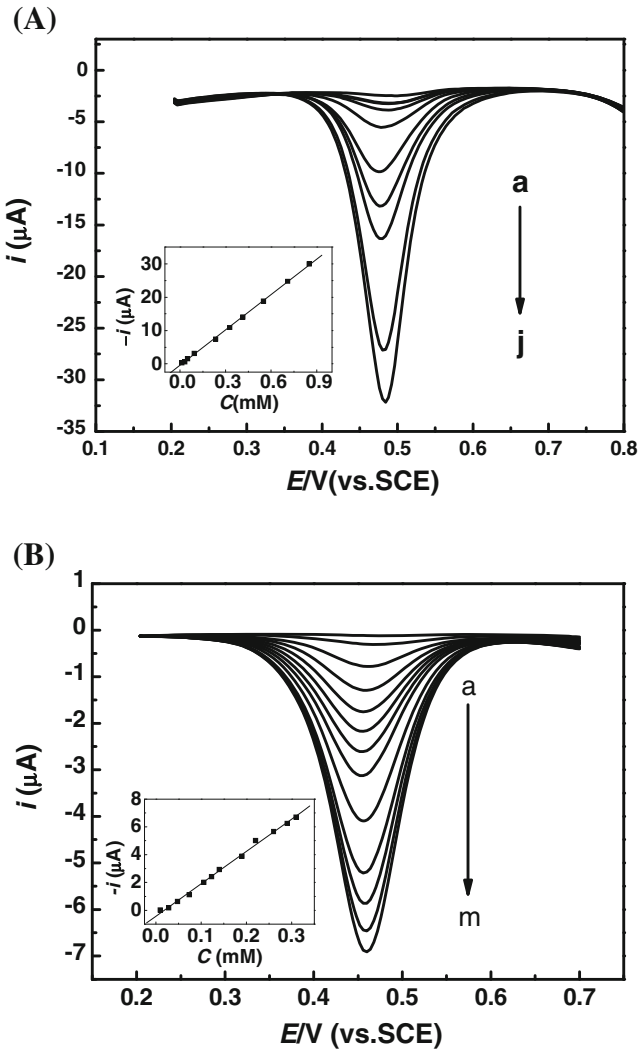

Fig. 9 **a** DPV obtained at N-CNTs/gold-modified GCE in pH 6.0 PBS containing 12, 31, 50, 93, 235, 327, 413, 550, 708.7, and 850 μmol L^{-1} of TH. **b** DPV obtained at N-CNTs-modified GCE in pH 6.0 PBS containing 9.5, 28, 48, 74, 106, 123, 140, 190, 220, 260, 290, and 310 μmol L^{-1} of TH. *Inset* relationship between the peak current and the concentration of TH

electrochemical process of TH. Furthermore, the peak current is linearly increased to scan rates in the range of 100 to 450 mV/s, which shows surface-controlled process for the oxidation of TH on the surface of the modified electrode.

Differential pulse voltammograms (DPV) has much higher sensitivity and resolution than CV, because the charge current to the background current is negligible in DPV. Figure 9a shows the DPV results using N-CNTs/gold-modified GCE in N_2-saturated 0.1 M pH 6.0 PBS upon addition of TH. Different concentrations of TH solution were successively added to 10 mL of buffer solution. To mix the added TH, intense stirring was kept for more than 0.5 min. After the stirring was stopped, CV was performed until the currents did not change any more, and then DPV was immediately carried out. The peak current of N-CNTs/gold-modified GCE increased with the increasing concentration of TH. The linear calibration range for TH is 12~850 μM (inset of Fig. 9a) with a detection limit of 1.3 μM at a signal-to-noise ratio of 3. DPV results obtained at N-CNTs-modified GCE in pH 6.0 PBS containing 9.5, 28, 48, 74, 106, 123, 140, 190, 220, 260, 290, and 310 μmol L^{-1} of TH are shown in Fig. 9b. The linear calibration range for TH is 9.5~310 μM (inset of Fig. 9b) with a detection limit of 7.2 μM. The corresponding linear range and detection limit of TH for pure CNTs-modified GCE are 20~280 μmol L^{-1} and 8.6 μM (the figure is not shown here), respectively. These results are in good agreement with the result of CVs.

In the previous work, Co nanoparticles-modified pure CNTs were used for voltammetric determination of TH [29]. The corresponding linear range was 50~100 μM with a detection limit of 5.0×10^{-8} M. Compared with our work, the reported detection limit was lower than that of our experiment but the linear range of TH for N-CNTs/gold-modified GCE was wider than this reported data which might be caused by the different detection systems.

The effect of possible interfering species on TH detection was examined using 1.0×10^{-5} M glucose, ascorbic acid, and uric acid, which caused an increase of 2.4%, 4.6%, and 3.9% in the oxidation current of 1.0×10^{-4} M TH, respectively. This result suggested that the proposed TH detection system had high anti-interference ability from those coexisted electroactive substances. The stability and reproducibility of the N-CNTs/gold composites-modified electrode was also studied. The relative standard deviation (RSD) was 2.8% for six successive determinations. The fabrication of five electrodes made independently showed an acceptable reproducibility with RSD of 5.2% for the current determined in the presence of 1.0×10^{-4} M TH. The long-term stability of the electrode was investigated over a 10-day period. When the modified electrodes were stored in pH 7.0 PBS or dried in air at 4 °C and measured every day, no obvious change was found.

Conclusions

In this work, N-CNTs/gold NPs composites were synthesized through simple self-assembly method. The morphology, composition, and optical properties of the resulted composites were investigated by TEM, SEM, Raman, UV–Vis, and XPS. This nanocomposite combines the advantages of N-CNT and Au NPs showing many excellent properties such as good solubility, dispersibility in water, and satisfactory biocompatibility. Based on these aspects, it was a modified electrode and applied to the voltammetric determination of TH successfully.

Acknowledgments This work is supported by the National Natural Science Foundation of China (Nos. 20905038, 20905010, 21073084, and 20773065) and Natural Science Foundation of Jiangsu Province (Nos. 08KJB150011).

References

1. Iijima S (1991) Nature 354:56–58
2. Rosen R, Simendinger W, Debbault C, Shimoda H, Fleming L, Stoner B, Zhou O (2000) Appl Phys Lett 76:1668–1670
3. Biercuk MJ, Llaguno MC, Radosavljevic M, Hyun JK, Johnson AT, Fischer JE (2002) Appl Phys Lett 80:2767–2769
4. Liang W, Bockrath M, Bozovic D, Hafner JH, Tinkham M, Park H (2001) Nature 411:665–669
5. Bachtold A, Hadley P, Nakanishi T, Dekker C (2001) Science 294:1317–1320
6. An KH, Kim WS, Park YS, Moon JM, Bae DJ, Lim SC, Lee YS, Lee YH (2001) Adv Funct Mater 11:387–392
7. Liu C, Fan YY, Liu M, Cong HT, Cheng HM, Dresselhaus MS (1999) Science 286:1127–1129
8. Rakhi RB, Sethupathi K, Ramaprabhu S (2009) J Phys Chem B 113:3190–3194
9. Valcárcel M, Cárdenas S, Simonet BM (2007) Anal Chem 79:4788–4797
10. Yue B, Ma YW, Tao HS, Yu LS, Jian GQ, Wang XZ, Wang XS, Lu YN, Hu Z (2008) J Mater Chem 18:1747–1750
11. Deng S, Jian G, Lei J, Hu Z, Ju H (2009) Biosens Bioelectron 25:373–377
12. Jin C, Nagaiah TC, Xia W, Spliethoff B, Wang SS, Bron M, Schuhmann W, Muhler M (2010) Nanoscale 2:981–987
13. Xu XA, Jiang SJ, Hu Z, Liu SQ (2010) ACS Nano 4:4292–4298
14. Feng X, Mao C, Yang G, Hou W, Zhu J-J (2006) Langmuir 22:4384–4389
15. Zhang J, Gu M, Zheng T, Zhu J (2009) Anal Chem 81:6641–6648
16. Cui R, Huang H, Yin Z, Gao D, Zhu J (2008) Biosens Bioelectron 23:1666–1673
17. Lin CE, Chen KH, Hsiao YY, Liao WS, Chen CC (2002) J Chromatogr A 971:261–266
18. Wang RY, Lu XN, Wu MJ, Wang E (1999) J Chromatogr B 721:327–332
19. Kojlo A, Michalowski J, Wolyniec EB (2000) J Pharm Biomed Anal 22:85–91
20. Zhang Z, Ma J, Lei Y, Lu Y (2007) Talanta 71:2056–2061
21. Yan W, Feng XM, Chen XJ, Hou WH, Zhu J-J (2008) Biosens Bioelectron 23:925–931
22. Chen H, Yang Y, Hu Z, Huo KF, Ma YW, Chen Y (2006) J Phys Chem B 110:16422–16427

23. Sarma TK, Chowdhury D, Paul AJ (2002) J Chem Soc Chem Commun 10:1048–1049
24. Ghosh K, Kumar M, Maruyama T, Ando Y (2009) Carbon 47:1565–1575
25. Yang Q, Shuai L, Zhou JJ, Lu FC, Pan XJ (2008) J Phys Chem B 112:12934–12939
26. Chu H, Wang J, Ding L, Yuan D, Zhang Y, Liu J, Li Y (2009) J Am Chem Soc 131:14310–14316
27. Guo L, Peng Z (2008) Langmuir 24:8971–8975
28. Mirkin CA (2000) Inorg Chem 39:2258–2272
29. Shahrokhian S, Ghalkhania M, Adeli M, Amini MK (2009) Biosens Bioelectron 24:3235–3241